DALTON

Stereochemical and conformational features of ruthenium sulfoxide complexes: a molecular mechanics approach‡

Silvano Geremia* and Mario Calligaris†

Dipartimento di Scienze Chimiche, Università di Trieste, via L. Giorgieri 1, 34127 Trieste, Italy

Molecular mechanics force-field constants for ruthenium(II) sulfoxide complexes have been derived for the implementation of the AMBER force field. Stretching and bending constants were calculated by Badger's and Halgren's equations. Twenty-six parameters for sulfoxide, chlorine and metal atoms have been optimized to fit 836 experimental bond lengths and angles, using the Simplex method. Atomic charges have been calculated by the semiempirical method ZINDO/1. The goal was to rationalize the stereochemical and conformational features of this kind of metal complexes, through an accurate description of the molecular structures. The accuracy of the resulting geometries is reflected in the low values of the average differences between observed and calculated bond lengths and angles (−0.007 Å and 0.0°) and their root-mean-square-deviations (0.017 Å and 1.3°). Conformational analyses for S- and O-bonded sulfoxides have been carried out. Possible rotamer distributions for ruthenium(II)–dimethyl sulfoxide complexes containing lopsided nitrogen ligands, arising from hindered rotation about the Ru–N bonds, also have been investigated.

Ruthenium complexes containing sulfoxide ligands present many stereochemical questions, because of the possibility of forming different linkage (S- and O-bonded species) and geometric isomers (*e.g. cis-trans*, *fac-mer* arrangements) as well as conformational isomers.[1] As to the bonding mode, available data indicate that S-bonding is preferred if the electron density on the metal centre is high enough to ensure a π-back bonding contribution in the metal–sulfur bond.[1] O-Bonding can be favoured by increasing the metal oxidation state, introducing strong π-acceptor ligands or by steric effects in the case of bulky sulfoxides. While dimethyl sulfoxide (dmso) yields a complex of formula *mer*,*cis*-[$RuCl_3$(dmso-*S*)$_2$(dmso-*O*)], diphenyl sulfoxide (dpso) gives *mer*,*cis*-[$RuCl_3$(dpso-*O*)$_2$(dpso-*S*)].[2] Molecular mechanics (MM) calculations have shown that the latter isomer is preferred over other possible ones, since it has the lowest strain energy, associated with the highest conformational entropy.[2]

Recently, restricted rotation of aromatic nitrogen ligands about Ru–N bonds in dmso complexes has been investigated extensively in solution through NMR techniques.[3,4] So, for instance, for *cis*,*cis*,*cis*-[$RuCl_2$(dmso-S)$_2$(dmim)$_2$] (dmim = 1,2-dimethylimidazole), four rotamers (**R1**–**R4**), in slow equilibrium at room temperature, have been detected in chloroform solution. They differ in the relative orientation of the lopsided nitrogen ligands, which can assume either head-to-head (h.h.) or head-to-tail (h.t.) conformations.[3] Ruthenium complexes with imidazole ligands are also of interest for their antitumour activity,[5] their ability to ligate radiosensitizing agents to DNA,[6] and their immunosuppression properties.[7] Understanding of the factors that influence the conformational properties of complexes containing two lopsided ligands in *cis* positions, such as substituted imidazoles, is fundamental for the elucidation of the mechanism of interaction of such metal complexes with biological systems. In this respect, it is of particular interest to investigate the stereochemistry of ruthenium–sulfoxide complexes, in view of their promising antitumour properties,[8] and especially of those containing also nitrogen ligands, as models for the covalent interactions of ruthenium with nucleic acids.[9]

Molecular mechanics calculations might allow the rationalization of the stereochemical and conformational behaviour of the above mentioned ruthenium(II)–sulfoxide complexes, provided a reliable force field were available. Unfortunately, no force field contains specific parameters for ruthenium complexes. Unlike organic and biological molecules, for which fairly complete force fields are available,[10–12] the use of MM in inorganic systems, even if well established,[13–17] is still limited by the requirement of highly element-specific forces fields. A 'universal' force field capable of describing a wide variety of metal-containing molecules has been described, but at this stage of development it does not possess the required accuracy.[18]

As is well known, the major problem in using MM with co-ordination compounds derives from the presence of strong electronic effects involving the metal atom, such as those related to co-ordination number, formal oxidation state, *trans* effects and π-bonding contributions. For these reasons and the relatively complicated atom labelling system, metal-specific force fields must be envisaged. In any case, a systematic problem in MM is the calculation of the force constants, especially for metal complexes, in view of the paucity of energetics and vibrational data. Another problem concerns the determination of the atomic charges in co-ordination compounds, so that, usually, the electrostatic contribution is neglected.[2]

To our knowledge, the only attempts at using MM for ruthenium complexes concern the structural characterization of the reaction product of *trans*-[$RuCl_2$(dmso-*S*)$_4$] with deoxyguanosine dinucleotide d(GpG),[19] and the study of the relative stability of the *mer*-[$RuCl_3$(dpso)$_3$] isomers.[2] In the former case, tentative force-field parameters for Ru^{II} were introduced in an AMBER force field.[20] In the second the TRIPOS 5.2 force field was used,[11] with the ruthenium(III) potential constants estimated from a few spectroscopic and structural data.[2]

In order partly to fill this gap and obtain deeper insight into the conformational aspects of octahedral ruthenium(II)–dmso complexes, we present here the derivation of a structure-optimized force field which can be used to simulate the structure of simple sulfoxide complexes of Ru^{II} as well as that of co-ordination compounds of Ru^{II} with molecules of biological interest. The AMBER force field has been selected,[12] imple-

* E-Mail: geremia@univ.trieste.it
† E-Mail: calligaris@univ.trieste.it
‡ *Supplementary data available* (No. SUP 57222, 16 pp.): final atom parameters. See Instructions for Authors, *J. Chem. Soc., Dalton Trans.*, 1997, Issue 1.
Non-SI unit employed: cal = 4.184 J.

mented with the introduction of the force-field parameters for the Ru^{II}–Cl–dmso groups and ligands of the pyridine and imidazole type.

Experimental

Force field

In AMBER[12] the molecular strain energy, E, is given by the sum of the deformation terms for the bond lengths (d), bond angles (θ) and dihedral angles (ψ) (including improper torsion angles which model out-of-plane displacements), together with the van der Waals and electrostatic contributions, equation (1)

$$E = \Sigma_b k^d (d - d^\circ)^2 + \Sigma_\alpha k^\theta (\theta - \theta^\circ)^2 + \{\Sigma_d V_n/2[1 + \cos(n\psi - \psi_\circ)]\} + \Sigma_{ij}[(a_{ij}/r_{ij}^{12}) - (b_{ij}/r_{ij}^{6}) + (q_i q_j/D r_{ij})] \quad (1)$$

where $a_{ij} = \delta(\varepsilon_i\varepsilon_j)^{\frac{1}{2}}(r^*_i + r^*_j)$ (ref. 12) and $b_{ij} = 2\delta(\varepsilon_i\varepsilon_j)^{\frac{1}{2}}(r^*_i + r^*_j)^6$, where r^* and ε are the van der Waals radii and the energy-well depth for two atoms of the same type, respectively, q is the atomic charge, D the relative permittivity. Electrostatic and van der Waals interactions are only calculated between atoms separated by at least three bonds. Non-bonded and electrostatic interactions between atoms separated by exactly three bonds are reduced by scale factors of 0.5 and 0.833, respectively; D can be a constant or a distance-dependent variable, $D = r_{ij}$.[12]

Energy calculations have been performed on a Pentium-90 personal computer using the HYPERCHEM 4.5 molecular modelling package.[21] The Polak–Ribiere version of the conjugate-gradient method has been used in all energy minimizations, till the convergence criterion of 0.001 kcal mol^{-1} $Å^{-1}$ was reached.

Force-field constants

Atom types for H and C atoms have been taken from AMBER,[12] while new atom types have been introduced for Ru^{II}, Cl, O–S (sulfoxide) and N (imidazole, pyridine), considering possible electronic *trans*-influence effects of S on the co-ordinated atoms (Table 1).[1]

As previously reported,[2] the potential constants for all the i–j bonds were calculated from Badger's rule,[22] $k^d_{ij} = 71.94[(A_{ij} - D_{ij})/(d^\circ_{ij} - D_{ij})]^3$, using the parameters proposed by Herschbach and Laurie,[23] when available, while those for the i–j–k bond angles were calculated from Halgren's equation,[24] $k^\theta_{ijk} = 125.9 Z_i C_j Z_k (d_{ij} + d_{ik})^{-1}(\theta^\circ_{ijk})^{-2}\exp[-2(d_{ij} - d_{jk})^2/(d_{ij} + d_{ik})^2]$. This approach allows an automatic variation of the stretching and bending constants as a function of the reference bond distances (d°_{ij}) and angles (θ°_{ijk}). Force-field constants k [or in our case, A, D, C and Z; hereafter, BH (Badger and Halgren) constants] and the d°, θ° parameters can be optimized with an iterative procedure, reducing the sum of the squares of the differences Δ between observed and calculated values, upon variation of the parameters.[25] In the present case the observables were the bond lengths and angles of 11 accurate crystal structures of ruthenium(II) complexes. Weights have been assigned to the experimental data, on the basis of their estimated errors, $w = 1/\sigma^2$. For the optimization procedure we adopted the Simplex method, in view of the non-linear nature of the equations and the facility for introducing restraints in the minimization.[26] Convergence was controlled by a goodness of fit parameter defined as $[\Sigma w\Delta^2/(n_{obs} - n_p)]^{\frac{1}{2}}$, where n_{obs} = number of observables and n_p = number of parameters. It was reached when the absolute relative difference between the lowest and the highest goodness of fit values was less than 0.0001. A local program in VISUALBASIC for WINDOWS was used for the calculation of the potential parameters and for the geometrical and Simplex calculations. This was linked to HYPERCHEM, so that the overall parameter optimization/energy minimization process could be run automatically.

Table 1 Atom types not included in AMBER

Atom	Type*	Description
Ru	RU2	Ruthenium(II)
S	SO	In O-bonded sulfoxides
	S*R*	In S-bonded sulfoxides, not *trans* to S
	SS*R*	In S-bonded sulfoxides, *trans* to S
Cl	CL*R*	Not *trans* to S
	CS*R*	*trans* to S
O	O1	In S-bonded sulfoxides
	OS*R*	In O-bonded sulfoxides
N	NIM	Unco-ordinated N in imidazole ligands
	NI*R*	Co-ordinated N in pyridine and imidazole ligands, not *trans* to S
	NS*R*	Co-ordinated N in pyridine and imidazole ligands, *trans* to S
	N3*R*	Co-ordinated ammonia

* *R* = X, Y and Z, depending on the atom position along the axes of a Cartesian system centred on the octahedral metal atom.

Van der Waals parameters for C, H, N and O were taken from AMBER,[12] and held fixed, as were the BH constants for the non-ruthenium interactions.[22,24] Van der Waals parameters for Ru, Cl and S, together with the BH constants for the ruthenium interactions and the corresponding 'unstrained' bond lengths and angles, have been refined. Starting values for BH and van der Waals parameters were taken from previous work,[2] while for d° and θ° average literature values were assumed.[1] Torsional barriers around C–C and C–N bonds were calculated as in AMBER.[12] Barriers around co-ordination bonds were not considered.[13]

The observed bond lengths and, particularly, the co-ordination bond angles can be slightly modified by packing effects, which can force the molecule into a strained conformation. In order to simulate crystal-packing effects, the torsional angles around single bonds and involving non-H atoms were constrained by a 16 kcal mol^{-1} energy barrier in the energy minimization to maintain the crystal structure conformation.

For the electrostatic contribution, atomic charges were calculated by the semi-empirical ZINDO/1 method, suitable for molecular orbital (MO) calculations of second-row transition-metal complexes, included in HYPERCHEM 4.5.[21] Charges on chemically equivalent atoms were averaged over all the equivalent ligands and assigned to the 11 input molecules. The ruthenium atom charges were such as to give the net charge of the complex. All charges were held fixed during the optimization procedure. Fig. 1 shows a sketch of the different molecular fragments with atom types and their atom and total ligand charges. The vacuum value ($D = 1$) was initially assumed for the relative permittivity, in view of future work on the solution conformational behaviour with explicit introduction of solvent molecules.[12,20] However, it was refined since the inclusion of the relative permittivity in the optimization process assures proper scaling of the electrostatic contribution. The final value of 7.9 is consistent with the fact that we are considering solid-state and not gas-phase structures. Final values of the refined parameters are in Table 2, together with the calculated stretching and bending constants. The force constants for the not-refined stretching and bending parameters (Table 3) were calculated using the literature BH constants.[24] At convergence the goodness of fit was 7.84 for $n_{obs} = 835$ and $n_p = 26$. Files with the final atom parameters (HIN format) have been deposited as SUP 57222.

Conformational analysis

The potential-energy surfaces for isolated molecules ($D = 1$) were explored using local EXCEL© MACRO functions, which allow minimization of the strain energy as the conformation of the molecule is varied through torsional angle rotations. In particular, the conformational analysis around a selected bond was performed with rotations of 5°, from −180 to 180°, introducing

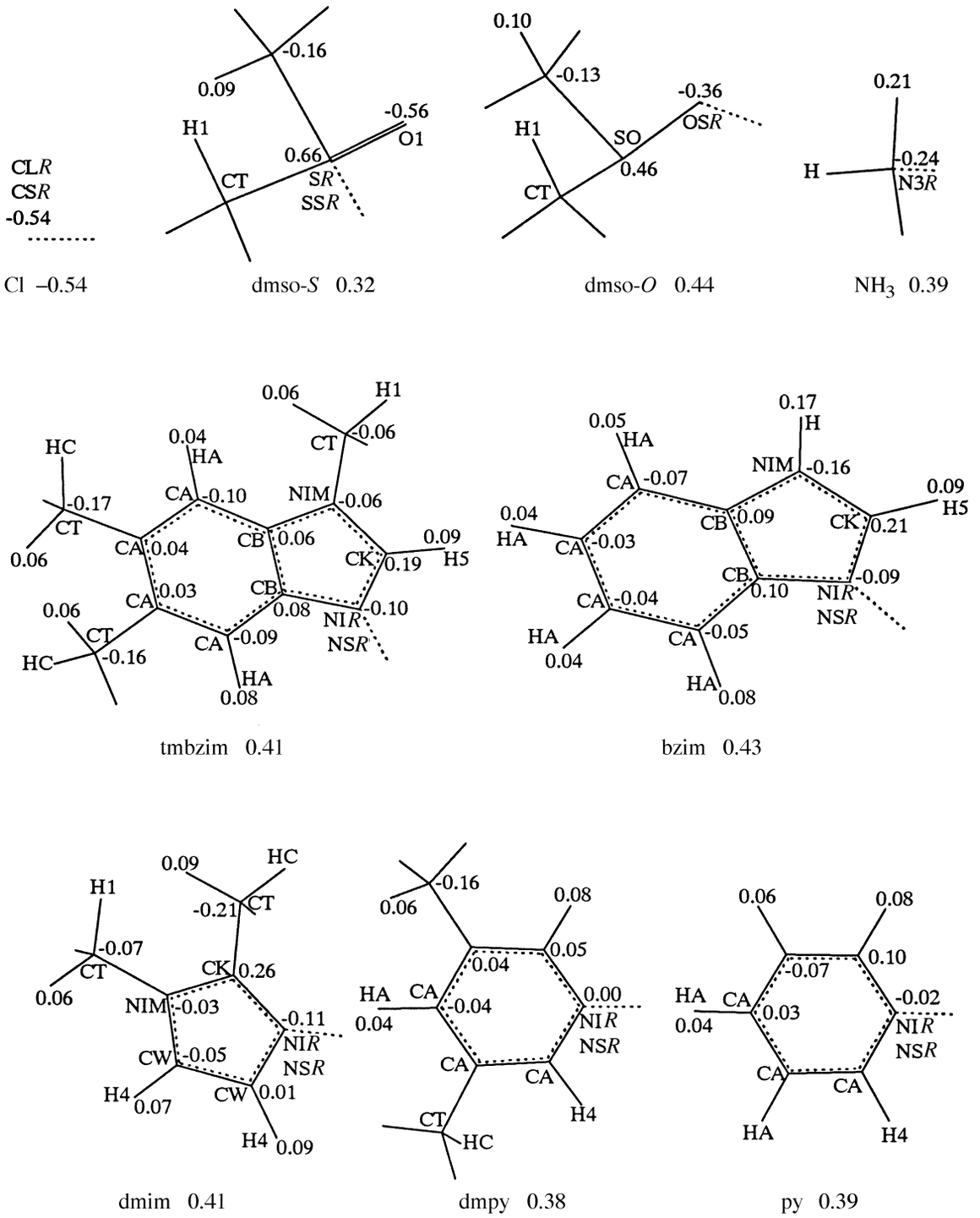

Fig. 1 Atom types and charges for the ligands in the Ru^{II}–dmso complexes. For equivalent atoms only one atom type and charge (e) is given. Total ligand charges are also shown

a constraint of 1000 kcal mol^{-1} to the current torsional angle, ψ. In order to find the absolute energy minimum for each ψ, the energy surface was thoroughly explored through a variation of all the remaining torsional degrees of freedom. In particular, the remaining torsional angles were rotated by 360° in steps of 60° and the relative energy minima found through a quick minimization of the strain energy with a convergence gradient of 0.1 kcal mol^{-1} $Å^{-1}$. The minimum-energy conformer was further minimized using a convergence gradient of 0.001 kcal mol^{-1} $Å^{-1}$. Final energy values for each ψ were then obtained by single-point energy calculations, without any restraint.

A distance-dependent relative permittivity was used for the investigation of the rotamer distribution in solution. It has been shown that, with the same force-field parameters, the passage from D = constant to $D = r_{ij}$ helps to compensate for the lack of explicit solvation by implicitly damping long-range charge interactions more than shorter-range ones.[12,20]

Results and Discussion

Validation of the force field

The consistency of the force field can be evaluated from the average values of the differences Δ between observed and calculated bond lengths and angles and their root-mean-square deviations, r.m.s. = $[(\Sigma\Delta^2)/n]^{\frac{1}{2}}$. Deviation from zero of the average values gives a measure of the asymmetry of the Δ distribution or indicates the presence of systematic errors, while r.m.s. gives

Table 2 Optimized force-field constants [A (Å), D (Å), C, Z, ε (kcal mol^{-1}), r^* (Å), d° (Å), θ° (°)], and related stretching and bending constants [k^d (kcal mol^{-1} Å^{-2}), k^θ (kcal mol^{-1} rad^{-2})]

BH and van der Waals constants

A_{Ru_2}	3.032	ε_{Cl}	0.492
D_{Ru_2}	1.124	r^*_{Cl}	1.850
C_{Ru}	0.33	ε_s	0.377
Z_{Ru}	1.39	r^*_s	1.746
ε_{Ru}	0.604	D	7.9
r^*_{Ru}	2.770		

Stretching constants	k^d	d°		k^d	d°
RU2–N3*R*	128.2	2.135	RU2–CL*R*	233.9	2.412
RU2–N1*R*	152.4	2.081	RU2–CS*R*	225.9	2.427
RU2–NS*R*	139.6	2.108	RU2–SO*R*	358.5	2.241
RU2–OS*R*	130.6	2.129	RU2–SS*R*	283.5	2.332

Bending constants[a]	k^θ	θ°		k^θ	θ°
CL*R*–RU2–CL*R*	7.0	180	NIX–RU2–SOY	31.2	90
CL*R*–RU2–NI*R*	7.0	180	NIX–RU2–SSY	30.5	90
CS*R*–RU2–SO*R*	7.7	180	NSX–RU2–NSY	28.5	90
N3*R*–RU2–SO*R*	7.7	180	NSX–RU2–OSY	33.1	90
NI*R*–RU2–NI*R*	7.2	180	NSX–RU2–SOY	31.1	90
NS*R*–RU2–SO*R*	7.8	180	NSX–RU2–SSY	30.3	90
OS*R*–RU2–SO*R*	9.0	180	OSX–RU2–OSY	38.5	90
SS*R*–RU2–SS*R*	8.2	180	OSX–RU2–SOY	36.1	90
CLX–RU2–CSY	28.1	90	OSX–RU2–SSY	35.3	90
CLX–RU2–NSY	28.0	90	SOX–RU2–SOY	34.0	90
CLX–RU2–OSY	32.6	90	SOX–RU2–SSY	33.3	90
CLX–RU2–SOY	30.9	90	SSX–RU2–SSY	32.7	90
CLX–RU2–SSY	30.3	90	RU2–NI*R*–C[b]	26.9	122.4
CSX–RU2–CSY	28.0	90	RU2–NS*R*–C[b]	26.6	122.4
CSX–RU2–N3Y	27.8	90	RU2–OS*R*–SO	38.0	120.9
CSX–RU2–NIY	28.0	90	RU2–SO*R*–CT	34.4	110.9
CSX–RU2–NSY	27.9	90	RU2–SS*R*–CT	33.3	110.9
CSX–RU2–OSY	32.5	90	RU2–SO*R*–O1	38.4	118.6
CSX–RU2–SOY	30.7	90	RU2–SS*R*–O1	36.9	118.6
CSX–RU2–SSY	30.2	90	RU2–N3*R*–H	18.0	109.5
N3X–RU2–SOY	30.9	90	CA–N[c]–CA	76.5	115.2
N3X–RU2–SSY	30.2	90	CB–N[c]–CK	75.2	115.2
NIX–RU2–NIY	28.8	90	CK–N[c]–CW	75.7	115.2
NIX–RU2–NSY	28.7	90	CT–S[d]–O1	101.9	107.7
NIX–RU2–OSY	33.3	90			

[a] X, Y, can be changed into X, Z, and Y, Z, for the *cis* positions. [b] CA, CB, CK and CW. [c] NI*R* and NS*R*. [d] SO*R* and SS*R*.

a measure of the spread of the Δ values and hence of the fit between calculated and experimental structures. The agreement between observed and calculated values appears to be quite good. The average differences for the whole data set of bond lengths and angles are −0.007 Å and 0.0°, respectively, with r.m.s. 0.017 Å and 1.3°. Mean and r.m.s. values are −0.002 Å, −0.1° and 0.013 Å, 1.6° considering only the ruthenium parameters. A reduction of the distance deviations and an increase of the angular deviations in the observables involving Ru can reflect a greater accuracy of the co-ordination bond lengths and higher flexibility of the co-ordination bond angles. Table 4 gives average differences and r.m.s. values for each of the 11 complexes. Differences between observed and calculated values appear quite acceptable, especially if we consider that the experimental values may be affected by several errors, deriving from the diffraction data quality (crystal quality), thermal motion effects, and residual packing and electronic effects. When there are two crystallographically independent species,[27,28] or in presence of independent structure determinations,[29,31] or in the case of polymorphs,[29] the experimental differences between chemically equivalent parameters can be even larger (Table 5) than those involving calculated values (Table 4). Finally, it is noteworthy that there is a significant increase in the convergence goodness of fit value (8.23), going from constrained to unconstrained energy minimizations. This reflects essentially on the r.m.s. of the angles involving the metal atom (1.8°) and suggests that packing effects play a role in the co-ordination angle deformations.

Besides the general agreement between the observed and calculated structures, the validity of the present force field is further shown by its ability to reproduce the angular deformations around the metal centre. It is remarkable that practically all the distortions from 90° of the X–Ru–Y angles are well reproduced. For only a few angles (4.2%) the sign of the deviation from 90° is not correctly predicted, but for only one N–Ru–N angle in **6**, the difference from 90° of the calculated value is as large as 2.7°. Of particular relevance, then, is the good reproducibility of the deformations of the Ru–N–C bond angles for the co-ordinated lopsided N-ligands. In **1** the two observed Ru–N–C bond angles for pyridine (py) are nearly equal, 120.6 and 122.7°, while for 1,5,6-trimethylbenzimidazole (tmbzim) the angles are 123.2 and 131.4°. The calculated values are in excellent agreement, being 120.3, 122.2, 123.2 and 132.4°, respectively. A fairly good agreement is also found in **2**, where for the two tmbzim ligands the observed values are 118.6, 135.9 and 125.2, 128.5, *vs.* the calculated values 121.7, 134.3 and 123.2, 132.4°, respectively. Similarly in **3**, for tmbzim and dmim the observed and calculated bond angles are, respectively: 123.8, 130.5, 122.6, 131.1 and 123.4, 132.1, 121.5, 134.3°.

As a further test of the force field, we have 'calculated' the structure of *cis*,*cis*,*cis*-[$RuCl_2$(dmso-*S*)$_2$(dmpy)(dmim)] **12** (dmpy = 3,5-dimethylpyridine) which was not included in the previous set because of static disorder in the dmim ligand.[32] Excluding this group, the agreement between the observed and calculated values for the highest-occupancy conformer is very good. Average differences and r.m.s. values (in parentheses) for

the Ru–X and X–Y bond lengths and X–Ru–Y, Ru–X–Y and X–Y–Z bond angles are, respectively, −0.005 (0.008) and −0.015 (0.019) Å, and 0.1 (0.8), 0.0 (0.8) and 0.1 (1.3)°. All deformations from 90° of the co-ordination bond angles are correctly reproduced. Calculated angles, Ru–N–C, for the dmim ligand of 120.2 and 135.4° are also in agreement with the experimental values 121.0 and 134.5°.

Table 3 Calculated stretching and bending constants [k^d (kcal mol^{-1} Å^{-2}), k^θ (kcal mol^{-1} rad^{-2})] from not-refined BH and $d°$ (Å), θ° (°) values

	k^d	$d°$		k^d	$d°$
CA–H[a]	381.3	1.080	CB–NIM	390.3	1.380
CW–H4	381.3	1.080	CB–N[c]	358.7	1.400
CK–H5	381.3	1.080	CK–NIM	451.1	1.347
CT–H[b]	367.0	1.090	CK–N[c]	520.4	1.316
CA–CA	358.7	1.400	CT–NIM	270.5	1.471
CA–CB	352.8	1.404	CW–CW	455.2	1.345
CA–CT	234.1	1.510	CW–NIM	418.3	1.364
CB–CB	366.2	1.395	CW–N[c]	385.3	1.383
CK–CT	261.5	1.480	CT–SO	232.2	1.782
H–N3*R*	505.6	1.010	CT–S[d]	232.2	1.782
H–NIM	505.6	1.010	O1–S[d]	669.9	1.472
CA–N[c]	472.1	1.337	SO–OS*R*	534.9	1.529
	k^θ	θ°		k^θ	θ°
CA–CA–CA	66.7	120	CK–CT–HC	44.6	109.5
CA–CA–CB	66.6	120	H1–CT–H1	31.8	109.5
CA–CA–CT	64.0	120	H1–CT–NIM	48.0	109.5
CA–CA–H[a]	42.0	120	H1–CT–S[d]	44.9	109.5
CA–CA–N[c]	73.1	120	HC–CT–HC	31.8	109.5
CB–CA–HA	42.1	120	CW–CW–H4	43.5	120
H4–CA–N[c]	46.9	120	CW–CW–NIM	74.0	120
CA–CB–CB	66.8	120	CW–CW–N[c]	73.4	120
CA–CB–NIM	72.0	120	H4–CW–NIM	46.2	120
CA–CB–N[c]	71.5	120	H4–CW–N[c]	45.6	120
CB–CB–NIM	72.2	120	H–N3*R*–H	37.5	109.5
CB–CB–N[c]	71.7	120	CK–NIM–H	44.4	120
CT–CK–NIM	70.6	120	CB–NIM–H	43.5	120
CT–CK–N[c]	71.2	120	CB–NIM–CK	69.2	120
H5–CK–NIM	46.6	120	CB–NIM–CT	66.0	120
H5–CK–N[c]	47.4	120	CK–NIM–CT	66.7	120
NIM–CK–N[c]	80.7	120	CK–NIM–CW	69.6	120
CA–CT–HC	43.8	109.5	CT–NIM–CW	66.4	120

[a] H4 and HA. [b] H1 and HC. [c] NI*R* and NS*R*. [d] SO*R* and SS*R*.

Stereochemistry of sulfoxide co-ordination

Inspection of the structural available data for O-bonded dmso metal complexes has shown that nearly 70% of the compounds assume the so-called *trans-trans* conformation, while the remaining 30% are nearly equally distributed among the *trans-cis*, *cis-trans* and *cis-cis* arrangements, as defined by the two M–O–S–C torsion angles, ψ_1 and ψ_2.[1] It has been suggested that the *trans-trans* geometry is favoured by interligand steric interactions.[1] For any M–O–S–C group the *trans* geometry is defined by a ψ value between 90 and 270°, while the *cis* geometry has ψ values less than 90° or greater than 270°.[1] Since the two torsion angles are related by the bond angles around the S atom, we can express any geometry by just one torsion angle, having $\psi_1 = \psi_2 + 102.9°$, on the basis of the θ° values of Table 2. Therefore, the different arrangements can be defined as: (*i*) *trans-trans*, with ψ_1 between −167 and −90°; (*ii*) *cis-trans*, with ψ_1 between −90 and 13°; (*iii*) *cis-cis*, with ψ_1 between 13 and 90°; and (*iv*) *trans-cis*, with $\psi_1 \leqslant -167°$ or $\geqslant 90°$.

In order to find the relative stability of these geometries, we have analysed the trend of the strain energy *E* with rotation around the O–S bond in complex **10**, *cis*-[$RuCl_2$(dmso-*S*)$_3$(dmso-*O*)] (experimental values, $\psi_1 = -120.1$, $\psi_2 = 137.1°$). As shown in Fig. 2, the *trans-trans* geometry displays a flat energy profile over its whole range of ψ_1, while the *cis-cis* geometry has a narrow minimum around $\psi_1 = 60°$, *ca.* 4 kcal mol^{-1}

Table 5 Average differences between experimental equivalent bond distances (Å) and angles (°), with r.m.s. values in parentheses, found in compounds containing chemically equivalent, but structurally independent, species; X, Y, Z represent generic non-metal atoms

Complex	Ru–X	X–Y	X–Ru–Y	Ru–X–Y	X–Y–Z
8[a]	−0.003	0.028	0.1	−0.1	0.0
	(0.012)	(0.035)	(3.4)	(2.5)	(2.9)
9[b]	0.003	−0.002	0.2	0.2	0.0
	(0.012)	(0.014)	(1.3)	(1.1)	(1.1)
10[c]	−0.004	−0.008	0.0	0.4	−0.3
	(0.009)	(0.014)	(1.8)	(3.3)	(1.2)
11[d]	0.016	0.011		0.1	0.1
	(0.021)	(0.014)		(0.4)	(0.1)

[a] Ref. 27. [b] Ref. 28. [c] Ref. 29. [d] Differences between two independent structure determinations, refs. 29 and 31.

Table 4 Average differences between observed and calculated bond distances (Å) and angles (°) with r.m.s. values in parentheses, after constrained energy minimization; X, Y, Z represent generic non-metal atoms

	Complex	Ru–X	X–Y	X–Ru–Y	Ru–X–Y	X–Y–Z
1	*cis*-[$RuCl_2$(dmso-*S*)$_2$(py)(tmbzim)][a]	−0.008	−0.013	0.2	0.2	0.0
		(0.011)	(0.019)	(1.0)	(1.0)	(0.7)
2	*cis*-[$RuCl_2$(dmso-*S*)$_2$(tmbzim)$_2$][a]	−0.003	−0.012	0.0	−0.2	0.1
		(0.011)	(0.021)	(1.7)	(1.9)	(0.9)
3	*cis*-[$RuCl_2$(dmso-*S*)$_2$(tmbzim)(dmim)][b]	−0.010	−0.010	0.0	−0.3	0.0
		(0.013)	(0.017)	(1.3)	(1.4)	(0.9)
4	*trans*-[$RuCl_2$(dmso-*S*)$_2$(tmbzim)$_2$][b]	−0.001	−0.011	0.2	0.0	0.1
		(0.012)	(0.019)	(1.2)	(1.5)	(0.8)
5	*trans*-[$RuCl_2$(dmso-*S*)$_2$(bzim)$_2$][b]	−0.002	−0.009	−0.1	−0.1	0.0
		(0.013)	(0.020)	(1.1)	(1.2)	(1.1)
6	*cis*-[$RuCl_2$(dmso-*S*)$_2$(dmpy)$_2$][b]	0.000	−0.013	0.0	0.1	0.2
		(0.009)	(0.016)	(1.9)	(1.2)	(1.2)
7	*cis*,*fac*-[$RuCl_2$(dmso-*S*)$_3$(NH_3)][c]	0.010	0.004	−0.1	0.0	0.1
		(0.018)	(0.012)	(1.3)	(1.3)	(0.9)
8	*fac*-[$RuCl_3$(dmso-*S*)$_3$]$^-$[d]	0.000	0.019	−0.1	0.0	0.2
		(0.012)	(0.029)	(1.3)	(1.1)	(2.3)
9	*fac*-[Ru(dmso-*S*)$_3$(dmso-*O*)$_3$]$^{2+}$[e]	−0.007	−0.009	−0.5	−0.1	−0.1
		(0.012)	(0.017)	(1.9)	(2.2)	(1.7)
10	*cis*,*fac*-[$RuCl_2$(dmso-*S*)$_3$(dmso-*O*)][f]	0.004	−0.004	−0.1	0.0	−0.5
		(0.016)	(0.008)	(1.4)	(1.1)	(1.3)
11	*trans*-[$RuCl_2$(dmso-*S*)$_4$][g]	−0.005	−0.001	0.1	−0.2	0.4
		(0.009)	(0.015)	(0.5)	(3.6)	(0.4)

[a] Ref. 4. [b] E. Alessio, S. Geremia and E. Zangrando, unpublished work. [c] Ref. 30. [d] Anion 1, ref. 27. [e] Cation I, ref. 28. [f] Polymorph **F3**, ref. 29. [g] Ref. 29.

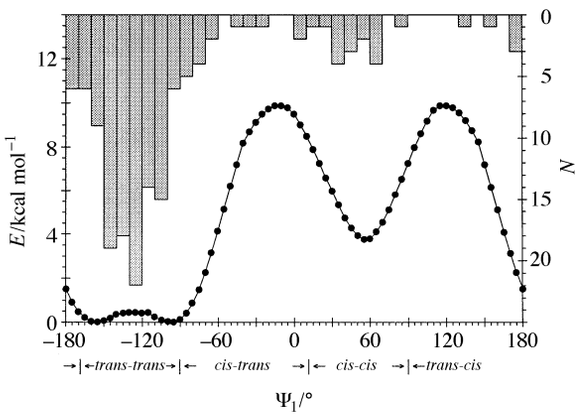

Fig. 2 Profile of the strain energy *E vs.* the torsion angle Ru–O–S–C ψ_1, for complex **10**, *cis*-[$RuCl_2$(dmso-*S*)$_3$(dmso-*O*)]. Superimposed on this plot is a histogram of the number of conformers of the known O-bonded sulfoxide metal complexes

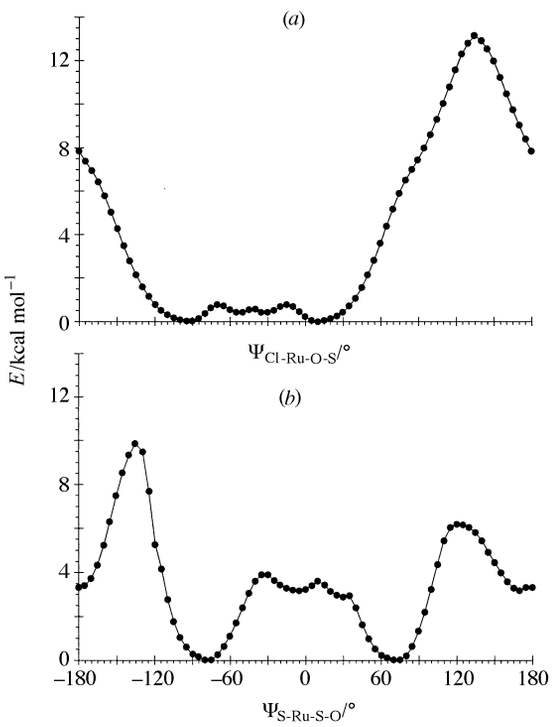

Fig. 3 Profiles of the strain energy *E vs.* the torsion angles ψ, Cl–Ru–O–S (*a*) and S–Ru–S–O (*b*) in *cis*-[$RuCl_2$(dmso-*S*)$_3$(dmso-*O*)] **10**

higher. The *trans-cis* and *cis-trans* arrangements have low-energy structures only when ψ_1 is close to −90 and −170°, respectively. In Fig. 2, superimposed on the *E vs.* ψ_1 plot, is shown a histogram of the number of conformers for the known O-bonded sulfoxide metal complexes.[1] The agreement between the two diagrams (lowest energy–largest occurrence) suggests that similar energy trends occur for the other complexes, in spite of the structural differences, confirming the steric interaction effects. In only a few cases, the *cis-cis* geometry is the favoured one.

Rotation about the Ru–O bond is essentially determined by the bulkiness of the *cis* ligands. In complex **10** the dmso-*O* group is pushed away from the bulkier *cis* dmso-*S* ligands toward the midpoint of the two *cis* Cl atoms [Cl(1)–Ru–O–S, ψ = −47.6°]. The energy profile [Fig. 3(*a*)] is characterized by a broad minimum between −120 and 40° with an energy barrier of *ca.* 14 kcal mol^{-1}.

The stereochemistry of the S-co-ordinated sulfoxides is characterized by the possible rotation about the M–S bonds, measured by the torsion angle X–M–S–O, ψ, where X is the *cis* ligand yielding the lowest torsion angle. It has been shown that, when only one S-ligand is present, its S–O bond tends to eclipse one co-ordination bond. In the case of more S-ligands, sulfoxides tend to assume staggered conformations with respect to co-ordination bonds.[1] For platinum(II) complexes containing *cis* S-bonded sulfoxides, it has been suggested that this arrangement could be due to electronic effects, allowing an increase of the overlap between the metal and ligand π orbitals.[33] On the other hand, it seems quite likely that the twisting around the M–S bond is determined by steric interactions, primarily among the metal-co-ordinated atoms and the sulfoxide alkyl or aryl groups. Owing to their greater bulk, these will tend to be staggered with respect to the co-ordination bonds forcing the O atom close to the co-ordination plane ($\psi \approx 0$ or 180°). In any case, many different conformations are feasible when more than one sulfoxide is present. Three polymorphs of **10** have been isolated so far (**F1**–**F3**), which, from the molecular point of view, are mere rotamers, as shown in Table VI of ref. 29. It is evident that **F1** and **F2** are very similar, while **F3** is significantly different, especially as regards the rotation around the Ru–S(3) bond, *e.g.* S(2)–Ru–S(3)–O(3) 9.2 in **F1**, 11.7 in **F2** and −70.5° in **F3**. The possibility of several conformations is confirmed by the MM calculations on **10**, analysing the energy trend for rotation around the Ru–S(3) bond. The *E vs.* ψ plot of Fig. 3(*b*) shows that the lowest minima occur at $\psi = \pm 80°$, while at an energy 3.2 kcal mol^{-1} higher three other minima are found at ψ = −5, 25 and 180°. The ψ value of the minimum at −80° is close to that of the torsion angle of **F3** , while those of **F1** and **F2** are not far from the −5 and 25° minima. Interestingly, polymorph **F3** is the most stable in the solid state,[2] suggesting that its stability is essentially determined by the intramolecular energy, rather than by packing effects.

Finally, comparison of Figs. 2 and 3 suggests that in O-bonded sulfoxide complexes the number of low energy occupied states is much larger than in S-bonded complexes. Both Figs. 2 and 3(*a*), considering the two degrees of rotational freedom around the Ru–O and O–S bonds of O-bonded dmso, show rather wide minima, while the conformational analysis around the Ru–S bond [Fig. 3(*b*)] evidences markedly narrower energy holes. This is in agreement with the hypothesis that O-bonded structures may be favoured by conformational entropy contributions.[2]

Restricted rotation of nitrogen bases

As mentioned above, in complex **12** the dmim ligand has been found to be disordered in the solid state, occupying two positions at 180° to each other, in the approximate molar ratio of 1.86 : 1.[32] This suggests the possible existence of two rotamers differing slightly in energy. Some NMR investigations in chloroform solution showed the presence of two rotamers, but with an inverse order of stability, the two species being in the ratio of 0.67 : 1 at room temperature.[32] The MM calculations are in agreement with these observations giving two minimum-energy structures. Using $D = 7.9$ the conformer with the lowest energy corresponds to that with highest occupancy in the crystal structure. The energy difference of 0.26 kcal mol^{-1} between the two conformers yields a population ratio, at room temperature, of 1.54 : 1, in good agreement with the solid-state value. Using a distance-dependent relative permittivity ($D = r_{ij}$), the MM calculations show the inverse order of stability, with an energy difference of 0.50 kcal mol^{-1} corresponding to a molar ratio of 0.44 : 1, comparable to the NMR data.

Furthermore, the application of the present force field to the conformational analysis of *cis*,*cis*,*cis*-[$RuCl_2$(dmso-*S*)$_2$(dmim)$_2$][3] **13**, mentioned in the introduction, shows the presence of four energy minima, confirming the experimental evidence for four main rotamers in solution. Calculations using $D = 7.9$, obtained from the refinement of the solid-state data, give the relative energies of the four rotamers (**R1**, 0.00; **R2**,

0.14; **R3**, 1.56; **R4**, 1.57 kcal mol^{-1}) which are not consistent with the solution population trend (**R1**:**R2**:**R3**:**R4** = 1.5:3.4:1.5:1).[3] It is interesting that again the use of a distance-dependent relative permittivity gives relative energies (**R1**, 0.60; **R2**, 0.00; **R3**, 0.89; **R4**, 1.31 kcal mol^{-1}) in better agreement with the solution results.[3]

Conclusion

The results of the present work show that force constants can be obtained from X-ray structural data, through the use of Badger's and Halgren's equations, associated with an optimization procedure, yielding a force field consistent with the crystal structure. Inclusion of the relative permittivity in the optimization process assures the proper scaling of the electrostatic energy contribution. Atomic charges for transition-metal complexes can be obtained by semiempirical MO calculations through the ZINDO/1 method.

As shown in Table 4, the present force field can simulate Ru–dmso molecular structures with good accuracy. In comparison, the TRIPOS 5.2 force field gives for small organic molecules average differences and r.m.s. deviations (in parentheses), for bond lengths and angles, respectively, of −0.011 (0.025) Å and −0.128 (2.50)°.[11]

However, we have seen that the energy differences calculated with D = a constant are not consistent with the rotamer distribution in solution. A better agreement is obtained with $D = r_{ij}$, but the population ratios for the different conformations are not well reproduced. This is not surprising since the force-field parameters have been optimized for structural and not energy data. Before we can expect to be able to reproduce the relative abundance of the different rotamers we need to take into account explicit solvent interactions and also conformational entropic contributions.[2]

Acknowledgements

Financial support from Ministero dell'Università e della Ricerca Scientifica e Tecnologica and Consiglio Nazionale delle Ricerche (Roma) is gratefully acknowledged. We are grateful to Dr. E. Alessio and Dr. L. G. Marzilli for helpful discussions.

References

1 M. Calligaris and O. Carugo, *Coord. Chem. Rev.*, 1996, **153**, 85.
2 M. Calligaris, P. Faleschini, F. Todone, E. Alessio and S. Geremia, *J. Chem. Soc., Dalton Trans.*, 1995, 1653.
3 M. Iwamoto, E. Alessio and L. G. Marzilli, *Inorg. Chem.*, 1996, **35**, 2384.
4 L. G. Marzilli, M. Iwamoto, E. Alessio, L. Hansen and M. Calligaris, *J. Am. Chem. Soc.*, 1994, **116**, 815; E. Alessio, M. Calligaris, M. Iwamoto and L. G. Marzilli, *Inorg. Chem.*, 1996, **35**, 2538.
5 M. J. Clarke, *Ruthenium and Other Non-platinum Metal Complexes in Cancer Chemotherapy*, Springer, Heidelberg, 1989, vol. 10; B. K. Keppler, *Metal Complexes in Cancer Chemotherapy*, VCH, Weinheim, 1993, p. 429.
6 M. McNamara and M. J. Clarke, *Inorg. Chim. Acta*, 1992, **195**, 175.
7 M. J. Clarke, V. M. Bailey, P. E. Doan, C. D. Hiller, K. J. LaChance-Galang, H. Daghlian, S. Mandal, C. M. Bastos and D. Lang, *Inorg. Chem.*, 1996, **35**, 4896.
8 G. Mestroni, E. Alessio, G. Sava, S. Pacor, M. Coluccia and A. Boccarelli, *Met.-Based Drugs*, 1994, **1**, 41; G. Mestroni, E. Alessio, G. Sava, S. Pacor and M. Coluccia, *Metal Complexes in Cancer Chemotherapy*, VCH, Weinheim, 1994, p. 159.
9 M. J. Clarke, B. Jansen, K. A. Marx and R. Kruger, *Inorg. Chim. Acta*, 1986, **124**, 13; F. Loseto, E. Alessio, G. Mestroni, G. Lacidogna, A. Nassi, D. Giordano and M. Coluccia, *Anticancer Res.*, 1991, **11**, 1549.
10 N. L. Allinger, Y. H. Yuh and J.-H. Lii, *J. Am. Chem. Soc.*, 1989, **111**, 8551.
11 M. Clark, R. D. Cramer III and N. Van Opdenbosch, *J. Comput. Chem.*, 1989, **10**, 982.
12 W. D. Cornell, P. Cieplak, C. I. Bayly, I. R. Gould, K. M. Merz, jun., D. M. Ferguson, D. C. Spellmeyer, T. Fox, J. W. Caldwell and P. A. Kollman, *J. Am. Chem. Soc.*, 1995, **117**, 5179.
13 G. R. Brubaker and D. W. Johnson, *Coord. Chem. Rev.*, 1984, **53**, 1.
14 A. Vedani and D. W. Huhta, *J. Am. Chem. Soc.*, 1990, **112**, 4759.
15 V. S. Allured, C. M. Kelly and C. R. Landis, *J. Am. Chem. Soc.*, 1991, **113**, 1.
16 P. V. Bernhardt and P. Comba, *Inorg. Chem.*, 1992, **31**, 2638.
17 M. Zimmer, *Chem. Rev.*, 1995, **95**, 2629.
18 A. K. Rappé, K. S. Colwell and C. J. Casewit, *Inorg. Chem.*, 1993, **32**, 3438.
19 G. Esposito, S. Cauci, F. Fogolari, E. Alessio, M. Scocchi, F. Quadrifoglio and P. Viglino, *Biochemistry*, 1992, **31**, 7094.
20 S. J. Weiner, P. A. Kollman, D. A. Case, U. Chandra Singh, C. Ghio, G. Alagona, S. Profeta, jun. and P. Weiner, *J. Am. Chem. Soc.*, 1984, **106**, 765.
21 HYPERCHEM, Hypercube, Inc., Waterloo, Ontario, 1994.
22 R. M. Badger, *J. Chem. Phys.*, 1934, **2**, 128; 1935, **3**, 70.
23 D. R. Herschbach and V. W. Laurie, *J. Chem. Phys.*, 1961, **35**, 458.
24 T. A. Halgren, *J. Mol. Struct.* (*Theochem.*), 1988, **163**, 431; *J. Am. Chem. Soc.*, 1990, **112**, 4710.
25 O. Ermer, *Struct. Bonding* (*Berlin*), 1976, **27**, 161.
26 P. C. Jurs, *Computer software applications in chemistry*, Wiley, New York, 1996.
27 R. S. McMillan, A. Mercer, B. R. James and J. Trotter, *J. Chem. Soc., Dalton Trans.*, 1975, 1006.
28 A. R. Davies, F. W. B. Einstein, N. P. Farrell, B. R. James and R. S. McMillan, *Inorg. Chem.*, 1978, **17**, 1965.
29 E. Alessio, G. Mestroni, G. Nardin, W. M. Attia, M. Calligaris, G. Sava and S. Zorzet, *Inorg. Chem.*, 1988, **27**, 4099.
30 M. Henn, E. Alessio, G. Mestroni, M. Calligaris and W. M. Attia, *Inorg. Chim. Acta*, 1991, **187**, 39.
31 J. S. Jaswal, S. J. Rettig and B. R. James, *Can. J. Chem.*, 1990, **68**, 1808.
32 L. G. Marzilli, E. Alessio, R. Roppa and E. Zangrando, unpublished work.
33 V. Yu. Kukushkin, V. K. Belsky, V. E. Konovalov, G. A. Kirakosyan, L. V. Konovalov, A. I. Moiseev and V. M. Tkachuk, *Inorg. Chim. Acta*, 1991, **185**, 143.

Received 11*th November* 1996; *Paper* 6/07647E